ELSEVIER

Remote Sensing of Environment 80 (2002) 435–446

Remote Sensing of Environment

www.elsevier.com/locate/rse

Assessing the information content of multiangle satellite data for mapping biomes II. Theory

Y. Zhang*, N. Shabanov, Y. Knyazikhin, R.B. Myneni

Department of Geography, Boston University, 675 Commonwealth Avenue, Boston, MA 02215, USA

Received 9 January 2001; received in revised form 4 September 2001; accepted 15 September 2001

Abstract

The insights gained from present land cover classification activities suggest integration of multiangle data into classification attempts for future progress. Land cover types that exhibit distinct signatures in the space of remote sensing data facilitate unambiguous identification of cover types. In this two-part series, we develop a theme for consistency among cover type definitions, uniqueness of their signatures, and physics of the remote sensing data. In the first part, Zhang et al.'s [Remote Sens. Environ., in press.] empirical arguments in support of the consistency principle were presented. This part provides a theoretical justification of the consistency requirements. Radiative transfer best explains the physics of the processes operative in the generation of the signal in the optical remote sensing data. Biome definitions given in terms of variables that this theory admits and the use of the transport equation to interpret biome signatures guarantee the consistency requirements. It is shown in this paper that three metrics of the biome angular signature in the spectral space — location, angular signature slope (ASSI), and length (ASLI) indices — are related to eigenvalues and eigenvectors of the transport equation. These variables allow a novel parameterization of canopy structure based on the partitioning of the incident radiation among canopy absorption, transmission, and reflection. Consistency between cover type definitions and uniqueness of their signatures with the physics of the remote sensing data is required not only to reduce ambiguity in land cover identification, but also to directly relate land cover type to biophysical and biogeochemical processes in vegetation canopies.

1. Introduction

The solar radiation reflected by a vegetation canopy and measured by satellite-borne sensors results from interaction of photons traversing through the foliage medium, bounded at the bottom by a radiatively participating surface (soil, understory, etc.). To estimate the canopy radiation regime, three important variables must be correctly formulated (Ross, 1981). They are (1) the architecture of individual plant or tree and the stand; (2) optical properties of the vegetation elements; and (3) reflective properties of the ground beneath the canopy. Photon transport theory aims at deriving the solar radiation regime, both within the vegetation canopy and the exitant radiance, using the above-mentioned attributes as input data. The success of remote sensing of vegetation depends, to a high degree, on being able to formulate a particular remote sensing problem, e.g., identification of the land cover type or estimation of surface biophysical variables, in terms of the abovementioned variables. Photon transport theory provides the most logical linkage between a specific remote sensing problem and the physics of the processes operative in the generation of the signal in the optical remote sensing data. This idea underlies the principle of consistency between biome definitions and uniqueness of their signatures with the physics of remotely sensed data formulated in the first part of our two-part series (Zhang, Tian, Myneni, & Knyazikhin, in press). The objective of this paper is to provide a theoretical basis for the consistency requirement.

The transport equation in three spatial dimensions is the appropriate starting point for our arguments for a theory for land cover identification. The bidirectional reflectance distribution function (BRDF) is defined as the solution of the three-dimensional transport equation at the upper canopy boundary along upward directions. We start with the simplest case when reflectance of the ground below the vegetation is

* Corresponding author. Tel.: +1-617-353-8845; fax: +1-617-353-8399.
E-mail address: yuzhang@crsa.bu.edu (Y. Zhang).

0034-4257/01/$ – see front matter
PII: S0034-4257(01)00320-0

zero and define variables required to characterize the interaction and transport of photons within the canopy and to uniquely resolve the transport equation. The directional hemispherical reflectance (DHR) is the hemispherically integrated BRDF, and is used to define the location of remotely sensed data in the spectral space. Knyazikhin, Martonchik, Myneni, Diner, and Running (1998) precisely derived the dependence of DHR on wavelength and expressed it uniquely as a simple function of the wavelength-dependent leaf albedo and wavelength-independent canopy-specific eigenvalue of the transport equation. This was recently validated with field measurements by Panferov et al. (2001). The eigenvalue governs the shortwave energy conservation in vegetation canopies; that is, the partitioning of incident radiation among absorption, transmission, and reflection. Thus, the energy conservation law determines the location of reflectance data in the spectral space in the case of vegetation canopies with a dark background. Note that DHR is a standard product of the multiangle imaging spectroradiometer (MISR) (Diner, Beckert, et al., 1998; Martonchik et al., 1998) and moderate resolution imaging spectroradiometer (MODIS) (Justice et al., 1998; Lucht & Schaaf, 2000) data. Two metrics, angular signature slope and length indices (ASSI and ASLI, respectively), which characterize the angular and spectral signatures of vegetation canopies are related to the eigenvalue of the transport equation and their properties are discussed below.

The three-dimensional radiation field in a scattering and absorbing medium bounded at the bottom by a reflecting surface can be expressed in terms of solutions of two surface-independent subproblems: the radiation field calculated for the case of a completely absorbing surface below the medium and the radiation field in the same medium generated by anisotropic wavelength-independent sources located at the bottom of the medium (Knyazikhin et al., 1998; Marshak, Knyazikhin, Davis, Wiscombe, & Pilewskie, 2000). We use this property to extend our analysis to the general case of a reflecting background beneath the vegetation.

Our theoretical investigation is based on the assumption that the transport equation can describe the radiative regime in vegetation canopies. However, it has been indicated by many investigators that the transport equation in its original form (Ross, 1981) cannot describe the radiative regime in vegetation canopies because it does not account for the hot-spot effect, i.e., a sharp peak about the retrosolar direction (Knyazikhin, Marshak, & Myneni, 1992; Kuusk, 1985; Li & Strahler, 1992; Marshak, 1989; Myneni, Marshak, & Knyazikhin, 1991; Nilson, 1991; Verstraete, Pinty, & Dickenson, 1990). With a simple example, we demonstrate that the solution of the transport equation contains a singular component that was ignored in all previous studies on three-dimensional radiative transfer problems, leading to the erroneous statement on inapplicability of the transport equation. This component describes the hot-spot effect. This justifies the use of the transport equation as the basis for interpretation of remotely sensed data acquired over vegetated land surface.

2. Signatures of vegetation in the case of an absorbing ground

Consider a vegetation canopy confined to $0<z<H$. The surface $z=0$ and bottom $z=H$ constitute its upper and lower boundaries. The spectral composition of the incident radiation is altered from interactions with phytoelements. The magnitude of scattering by the foliage elements is characterized by the hemispherical leaf reflectance and transmittance, defined as follows: the hemispherical leaf transmittance (reflectance) is the portion of radiation flux density incident on a leaf surface that is transmitted (reflected). Their sum is denoted as the hemispherical leaf albedo. The reflectance and transmittance of an individual leaf depends on wavelength, tree species, growth conditions, leaf age, and its location in the canopy. For simplicity, leaf albedo is assumed to be spatially independent, and the ratio of leaf transmittance to leaf albedo independent of wavelength. We start with the simplest case — the reflectance of the ground below the vegetation is zero. Results presented in this section are required to extend our analysis to the general case of a reflecting ground below the vegetation. Let a parallel beam of intensity c_λ be incident on the upper boundary. The governing transport equation is

$$\Omega\cdot\nabla I_\lambda(r,\Omega)+u_L(r)G(r,\Omega)I_\lambda(r,\Omega)=\omega_\lambda u_L(r)\int_{4\pi}\frac{1}{\pi}\Gamma(r,\Omega'\to\Omega)I_\lambda(r,\Omega')\mathrm{d}\Omega', \quad (1)$$

and the boundary conditions are

$$I_\lambda(r_0,\Omega)=|\mu_0|^{-1}\delta(\Omega-\Omega_0),$$

for downward directions, (2)

$$I_\lambda(r_H,\Omega)=0, \qquad \text{for upward directions.} \quad (3)$$

Here, the vector r denotes the Cartesian triplet (x,y,z) with its origin at the canopy top; r_0 and r_H denote points on the upper and lower boundaries, respectively. The unit vector Ω is expressed in spherical coordinates with respect to $(-Z)$ axis and $\cos^{-1}\mu$ and ϕ are its polar angle and azimuth. $\Omega_0=(\mu_0,\ \phi_0)$ is the direction of the parallel beam; I_λ (in sr^{-1}) is the ratio of the monochromatic radiance at r in the direction Ω at wavelength λ to incident flux $c_\lambda|\mu_0|$, where $\cos^{-1}\mu_0$ is the solar zenith angle. u_L is the leaf area density distribution function. G is the projection of leaf normals at r onto a plane perpendicular to the direction Ω. The symbol Γ denotes the area scattering phase function normalized by the leaf albedo ω_λ. Given the assumption above regarding the leaf spectral transmittance and albedo, this variable does not depend on wavelength (Knyazikhin & Marshak, 1991). A precise description of variables used can be found in Myneni (1991) and Ross (1981). Below, the formulation of Myneni (1991) is adopted.

The BRDF is the directional radiance reflected from a target divided by the irradiance (incident flux) illuminating the target at a single incident angle (Nicodemus, Richmond, Hsia, Ginsberg, & Limperis, 1977). For a vegetation canopy bounded below by a black surface, the BRDF is the solution I_λ of the boundary value problem (Eqs. (1)–(3)). Note that I_λ depends on values of the spectral leaf albedo that in turn depend on wavelength. It allows the parameterization of BRDF in terms of leaf albedo rather than wavelength. Therefore, the wavelength dependence will be suppressed in further notations. The value of leaf albedo will be added to the argument list of the solution of Eqs. (1)–(3).

We investigate spectral and angular variation in BRDF using operator theory (Richtmyer, 1978; Vladimirov, 1963) by introducing the differential and integral operators (L and S operators, respectively; Eq. (4))

$$\begin{aligned} LI_\omega &= \Omega \cdot \nabla I_\omega + u_{\mathrm{L}}(r)G(r,\Omega)I_\omega(r,\Omega); \\ SI_\omega &= u_{\mathrm{L}}(r)\int_{4\pi}\frac{1}{\pi}\Gamma(r,\Omega'\to\Omega)I_\omega(r,\Omega')\mathrm{d}\Omega'. \end{aligned} \tag{4}$$

It should be emphasized that the differential and integral operators do not depend on leaf albedo. The solution I_ω of Eqs. (1)–(3) can be represented as the sum of two components, viz., $I_\omega = Q + \varphi_\omega$. Here, the wavelength-independent function $|\mu_0|Q$ is the probability density that a photon in the direct beam will arrive at r along Ω_0 without suffering a collision. It satisfies the equation $LQ = 0$ and the boundary conditions (Eqs. (2) and (3)). Note that Q contains the Dirac delta function $\delta(\Omega - \Omega_0)$, and thus, it takes zero values in all directions except Ω_0. The second term describes photons scattered one or more times in the canopy. It satisfies $L\varphi_\omega = \omega S\varphi_\omega + \omega SQ$ and zero boundary conditions. By letting $T = L^{-1}S$, the latter can be transformed to

$$\varphi_\omega = \omega T\varphi_\omega + \omega TQ. \tag{5}$$

Substituting $\varphi_\omega = I_\omega - Q$ into Eq. (5) results in an integral equation for I_ω (Bell & Glasstone, 1970; Vladimirov, 1963):

$$I_\omega - \omega TI_\omega = Q. \tag{6}$$

It follows from Eq. (6) that $I_\omega - \omega TI_\omega$ does not depend on ω and involves the validity of the following relationship

$$I_\omega - \omega TI_\omega = I_\alpha - \alpha TI_\alpha, \tag{7}$$

where I_ω and I_α are solutions of Eqs. (1)–(3) corresponding to leaf albedos ω and α, respectively.

An eigenvalue of the operator T is a number p such that there exists a function ψ that satisfies $\psi = pT\psi$. Kaufmann et al. (2000), Knyazikhin et al. (1998), and Panferov et al. (2001) defined the eigenvalue and eigenvector problem for the integro-differential form of the transport equation specified in Eq. (1) that is equivalent to the above formulation. Under some general conditions (Vladimirov, 1963), the sets of eigenvalues p_k ($k = 0, 1, 2, \ldots$) and eigenvectors $\psi_k(r,\Omega)$ ($k = 0, 1, 2, \ldots$) are a discrete set; the eigenvectors satisfy the condition of orthogonality. The transport equation has a unique positive eigenvalue that corresponds to a unique positive eigenvector. This eigenvalue is greater than the absolute magnitudes of the remaining eigenvalues. This means that only one eigenvector, say ψ_0, takes on positive values for any r and Ω. Fig. 1 shows an example of the positive eigenvector of T evaluated by the Kellogg's method (Riesz & Sz.-Nagy, 1990).

2.1. Location of canopy reflectances in spectral space

The location of reflectance data in spectral space is an important source of information about the vegetation canopy conveyed by multiangle and multispectral satellite data. The DHR, defined as

$$\mathbf{r}(\omega) = \left\langle \int_{2\pi} I_\omega(r_0,\Omega)|\mu|\mathrm{d}\Omega \right\rangle_0, \tag{8}$$

is used to specify the location of multiangle data. Here, $\langle\,\rangle_0$ denotes the average over the upper canopy boundary. Let $\mathbf{t}(\omega)$ and $\mathbf{a}(\omega)$ be canopy transmittance and absorptance corresponding to leaf albedo ω, i.e.,

$$\mathbf{t}(\omega) = \left\langle \int_{2\pi} I_\omega(r_{\mathrm{H}},\Omega)|\mu|\mathrm{d}\Omega \right\rangle_{\mathrm{H}}, \tag{9}$$

$$\mathbf{a}(\omega) = \frac{(1-\omega)\int_V \mathrm{d}r \int_{4\pi} u(r)_{\mathrm{L}}G(r,\Omega)I_\omega(r,\Omega)\mathrm{d}\Omega}{S}. \tag{10}$$

Here, $\langle\,\rangle_{\mathrm{H}}$ denotes the average over the canopy bottom, V is the domain in which the canopy is located, and S is area of

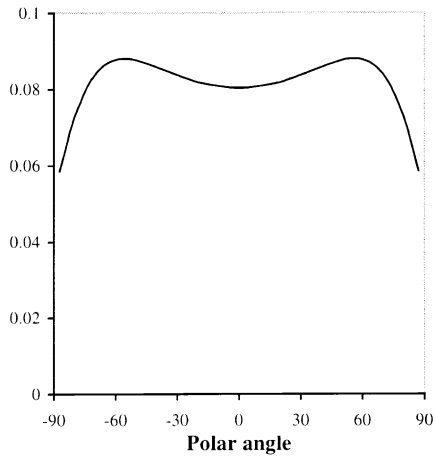

Fig. 1. Positive eigenvector $\varphi_0(r_0,\Omega)$ of the operator $T = L^{-1}S$ at the canopy top and in upward directions. Polar angles are shown with a positive (negative) sign if the azimuth of the upward direction is 0° (180°). The positive eigenvalue is $p = 0.785$. Calculations were performed for homogeneous canopy, $u_{\mathrm{L}}(r) = \mathrm{LAI}/H$, and uniform leaves, $G = 0.5$; $\Gamma(\upsilon) = (3\pi)^{-1}(1-\gamma)(\sin\upsilon - \upsilon\cos\upsilon) - \gamma\cos\upsilon/3$. Here, LAI is the leaf area index, υ is the scattering angle, and γ is the ratio of leaf transmittance to leaf albedo. LAI and γ were set to 4 and 0.46, respectively. In the case of uniform leaves, the eigenvector does not depend on azimuth.

the upper canopy boundary. Variables (Eqs. (8)–(10)) are related via the energy conservation law as

$$\mathbf{t}(\omega) + \mathbf{r}(\omega) + \mathbf{a}(\omega) = 1; \tag{11}$$

that is, the radiation absorbed, transmitted, and reflected by the canopy is equal to radiation incident on the canopy. Let $\mathbf{i}(\omega)$ be canopy absorption $\mathbf{a}(\omega)$ normalized by leaf absorption $1-\omega$, i.e.,

$$\mathbf{i}(\omega) = \frac{\mathbf{a}(\omega)}{1-\omega} = \frac{1-\mathbf{t}(\omega)-\mathbf{r}(\omega)}{1-\omega}. \tag{12}$$

For a vegetation canopy bounded at the bottom by a black surface, this variable is the average number of photon interactions with the leaves before either being absorbed or exiting the medium. We term this canopy interception.

Eq. (7) allows a relationship between the maximum eigenvalue p_0 and canopy interception to be established. Multiplying this equation by the extinction coefficient $\sigma = u_L G$ and integrating over V and all directions Ω results in

$$\mathbf{i}(\omega) - \omega q_i(\omega)\mathbf{i}(\omega) = \mathbf{i}(\alpha) - \alpha q_i(\alpha)\mathbf{i}(\alpha). \tag{13}$$

Here,

$$q_i(\omega) = \frac{\int_V \mathrm{d}r \int_{4\pi} u_L(r) G(r,\Omega)\psi_\omega \mathrm{d}\Omega}{\mathbf{i}(\omega)\cdot S}, \tag{14}$$

where $\psi_\omega = TI_\omega$ and I_ω is the solution of Eqs. (1)–(3). It can be shown that $q_{\mathbf{i}}(\omega) = p_0$, where p_0 is the positive eigenvalue of the operator T (Knyazikhin et al., 1998). This implies that the ratio (Eq. (14)) is invariant with respect to the wavelength, and the value of p_0 is determined by intrinsic structural properties of the vegetation canopy. Multiplying Eq. (7) by $|\mu|$, integrating over all downward directions and averaging over the canopy lower boundary, one obtains a similar relationship for canopy transmittance, with another wavelength-independent constant $p_{\mathbf{t}}$:

$$\mathbf{t}(\omega) - \omega p_t \mathbf{t}(\omega) = \mathbf{t}(\alpha) - \alpha p_t \mathbf{t}(\alpha). \tag{15}$$

Panferov et al. (2001) investigated the spectral-invariance property of canopy interception and transmission in the general case (i.e., without the previously mentioned assumption regarding the leaf optical properties) and confirmed it with field measurements. It was demonstrated that the variables p_0 and $p_{\mathbf{t}}$ govern the shortwave energy conservation in vegetation canopies; that is, the partitioning of incident radiation among canopy absorption, transmission, and reflection. A similar relationship, however, cannot be derived for canopy reflectances (Panferov et al., 2001), because $Q = 0$ for upward directions, and thus, the integration of Eq. (14) over upward traveling directions does not specify a wavelength-independent coefficient.

Thus, given p_0 and $p_{\mathbf{t}}$ and canopy interception ($\boldsymbol{i}(\alpha)$) and transmittance ($\mathbf{t}(\alpha)$) at a reference leaf albedo α, one can evaluate these variables for any leaf albedo. These variables, p_0, $p_{\mathbf{t}}$, $\mathbf{t}(\alpha)$, and $\mathbf{i}(\alpha)$, are determined solely by the structural properties of vegetation. The DHR can be evaluated via the energy conservation law (Eq. (11)). In the case of dense canopies, Eqs. (11), (13), and (15) determine the location of reflectance data in the spectral space as a function of leaf albedo and canopy structure. This facilitates the linkage between land cover type, expressed in terms of these variables, to biophysical and biogeochemical processes in vegetation canopies.

2.2. ASSI and ASLI

In terms of the transport theory, the BRDF is the solution φ_ω of Eq. (5) for diffuse radiation in upward directions and at the upper canopy boundary, i.e., $\mathrm{BRDF} = \langle \varphi_\omega(r_0,\Omega)\rangle_0$. To characterize the scattering process within the canopy, the following function is introduced (see Eq. (16)) (Kaufmann et al., 2000)

$$\eta_{n,\omega}(r,\Omega) = \frac{T^n \varphi_\omega}{\varphi_\omega}. \tag{16}$$

If the solution φ_ω is treated as a source within the vegetation canopy, $T^n\varphi_\omega$ describes the intensity of photons from this source scattered n times and attenuated by the vegetation canopy. $\eta_{n,\omega}$ is the ratio between the intensity of n times scattered and attenuated radiation to φ_ω. It follows from Eq. (5) that $0 \le \omega\eta_{1,\omega} \le 1$ at any spatial point and in any direction. The function $\eta_{1,\omega}$ is related to the eigenvalue p_0 as follows (Kaufmann et al., 2000; Knyazikhin, 1990; Krasnoselskii, 1964): the sequences,

$$a_n = \sqrt[n]{\inf \eta_{n,\omega}}, \quad b_n = \sqrt[n]{\sup \eta_{n,\omega}} \tag{17}$$

converge to the maximum eigenvalue p_0 of the operator T from below and above; that is, $a_n \le p_0 \le b_n$. The supremum and infinum in Eq. (17) are taken over all spatial points and directions for which $u_L(r) \neq 0$. Thus, the values of the function $\eta_{n,\omega}$ vary about ${p_0}^n$ and the interval $[a_n^n, b_n^n]$ of its variation becomes arbitrarily small as n tends to infinity.

The solution φ_ω can be expanded in Neumann series as (Knyazikhin & Marshak, 1991)

$$\begin{aligned}\varphi_\omega &= \omega TQ + \omega^2 T^2 Q + \omega^3 T^3 Q + \cdots + \omega^n T^n Q \\ &\quad + \omega^n T^n \left(\omega TQ + \omega^2 T^2 Q + \omega^3 T^3 Q + \cdots\right) \\ &= \omega TQ + \omega^2 T^2 Q + \omega^3 T^3 Q + \cdots + \omega^n T^n Q + \omega^n T^n \varphi_\omega \\ &= \omega TQ + \omega^2 T^2 Q + \omega^3 T^3 Q + \cdots + \omega^n T^n Q + \omega^n \eta_{n,\omega}\varphi_\omega.\end{aligned}$$

It follows from these relationships that

$$\varphi_\omega = \omega \frac{TQ + \omega T^2 Q + \omega^2 T^3 Q + \cdots + \omega^{n-1} T^n Q}{1 - \omega^n \eta_{n,\omega}}. \tag{18}$$

Eq. (18) establishes the required relationship between the BRDF and the eigenvalue of the operator T: for

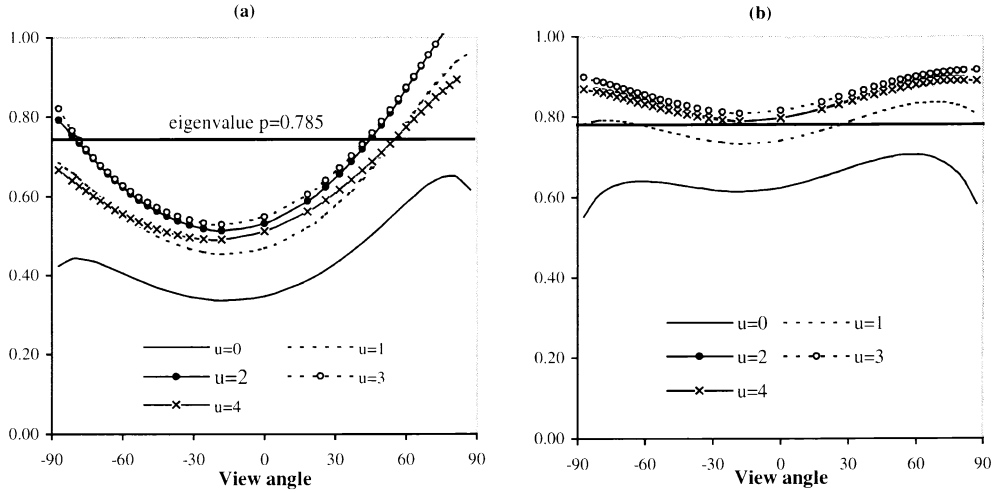

Fig. 2. Function $\eta_{1,\omega}$ at (a) red and (b) NIR wavelengths for various values of the cumulative leaf area index $u = \mathrm{LAI}\cdot z/H$. The solar zenith angle is 15°. Other parameters are the same as in Fig. 1. The eigenvalue $p_0 = 0.785$ of the operator T is shown as a bold straight line.

sufficiently large n, the function $\eta_{n,\omega}$ can be replaced with ${p_0}^n$. The function $\eta_{n,\omega}$ was introduced in Kaufmann et al. (2000) and used to assesses the effect of changes in solar zenith angle on reflectances in Channels 1 and 2 and normalized difference vegetation index (NDVI) from the AVHRR Pathfinder land data set. The theoretical and empirical analyses indicated that for dense canopies, $\eta_{1,\omega}$ is minimally sensitive to solar zenith angle changes and this sensitivity decreases as leaf area increases. If the reciprocity principle is valid for vegetated surfaces, this function should possess the same properties with respect to view angles, i.e., one may expect small variation in $\eta_{1,\omega}$ due to view angle changes. Fig. 2 shows the function $\eta_{1,\omega}$ at red ($\omega_{\mathrm{red}} = 0.2$) and near-infrared (NIR; $\omega_{\mathrm{NIR}} = 0.92$) spectral bands. We focus on Eq. (18) for $n = 1$ in our study. It should be noted, however, that this case might not provide a full interpretation of remotely sensed surface reflectances.

The BRDF can be expressed in terms of the function $\eta_{1,\omega}$ as

$$\varphi_\omega = \omega \frac{F}{1 - \omega\eta_{1,\omega}}. \tag{19}$$

Here, $F = TQ$ is the probability density that a photon from the direct beam, having been scattered by a phytoelement will escape the canopy. The probability density function F mainly determines the shape of BRDF. The ratio between BRDFs at NIR and red spectral bands, or the simple ratio (SR, Eq. (20)), results in the cancellation of F; thereby decreasing its sensitivity to view angle changes, i.e.,

$$\mathrm{SR}(\Omega) = \frac{\varphi_{\mathrm{NIR}}}{\varphi_{\mathrm{red}}} = \frac{\omega_{\mathrm{NIR}}}{\omega_{\mathrm{red}}} \frac{1 - \omega_{\mathrm{red}}\eta_{1,\mathrm{red}}}{1 - \omega_{\mathrm{NIR}}\eta_{1,\mathrm{NIR}}} \tag{20}$$

The POLDER (polarization and directionality of the Earth's reflectances) surface reflectances demonstrate this effect:

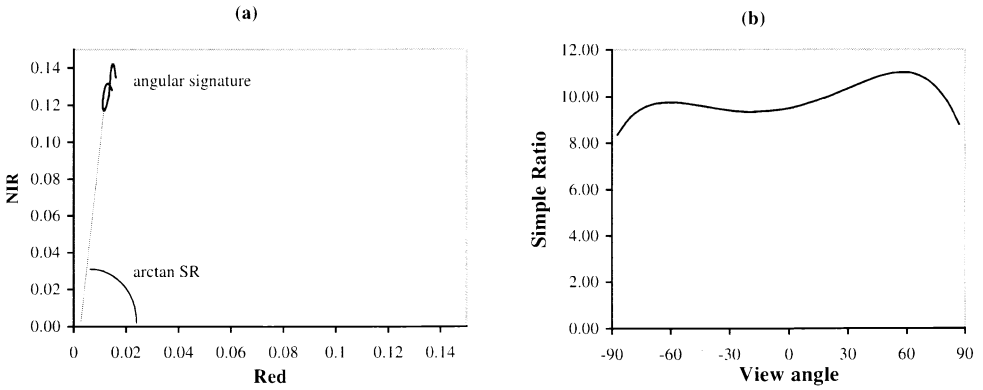

Fig. 3. (a) Angular signature of canopy reflectance on the red–NIR plane and (b) SR. All parameters were set to the same values as in Fig. 2. Arctangent of the SR is the angle between the line that connects a point on the signature and the origin of coordinates, and the horizontal axis. In this example, SR varies between its maximum (11.02) and minimum (8.37) values; its mean and standard deviation are 9.96 and 0.69, respectively. Thus, the linear function $\mathrm{BRDF}_{\mathrm{NIR}}(\Omega) = 9.96\cdot\mathrm{BRDF}_{\mathrm{red}}(\Omega)$ approximates the angular signature within uncertainty value of $0.69\cdot\mathrm{BRDF}_{\mathrm{red}}$ that corresponds to relative uncertainty $\delta\mathrm{BRDF}_{\mathrm{NIR}}/\mathrm{BRDF}_{\mathrm{NIR}} = 0.069$.

although some BRDFs exhibit a hot-spot-like behavior (Fig. 7 in Zhang et al., in press), their angular signatures in the spectral space are almost linear (Fig. 8 in Zhang et al., in press). Fig. 3 demonstrates another example of variation in BRDF and SR. Values of BRDFs at red and NIR spectral bands are related as $\mathrm{BRDF}_{\mathrm{NIR}}(\Omega)=\mathrm{SR}(\Omega)\cdot\mathrm{BRDF}_{\mathrm{red}}(\Omega)$. The coefficient $\mathrm{SR}(\Omega)$ is slightly sensitive to Ω and thus one can replace it by its mean value k. Based on the Minkowski inequality (Bronstein & Semendyayev, 1985), the following estimate of the accuracy (Eq. (21)) can be performed

$$\begin{aligned}\delta\mathrm{BRDF}_{\mathrm{NIR}} &= \int_{2\pi^+}[(\mathrm{SR}_{\mathrm{NIR}}(\Omega)-k)\cdot\mathrm{BRDF}_{\mathrm{red}}]^2\mathrm{d}\Omega\\ &\le \sqrt{\int_{2\pi^+}[\mathrm{SR}_{\mathrm{NIR}}(\Omega)-k]^2\mathrm{d}\Omega}\\ &\quad\times\sqrt{\int_{2\pi^+}\mathrm{BRDF}_{\mathrm{red}}^2\mathrm{d}\Omega}\\ &= \sigma\cdot\|\mathrm{BRDF}_{\mathrm{red}}\|, \end{aligned}\tag{21}$$

where σ is the standard deviation of the SR and $\mathrm{BRDF}^2_{\mathrm{red}}=\int_{2\pi^+}\mathrm{BRDF}^2_{\mathrm{red}}(\Omega)\mathrm{d}\Omega$. This explains the near-linear relationship between BRDFs at red and NIR spectral bands observed in POLDER data in the case of dense canopies.

Fig. 4 demonstrates the function $\omega\eta_{1,\omega}$ at the NIR spectral band derived from airborne multiangle imaging spectroradiometer (AirMISR) (Diner, Barge, et al., 1998) surface reflectance acquired over grassland, July 11–17, 1999 (Wang et al., 1999). The following relationship between the NDVI and $\eta_{1,\mathrm{NIR}}$ reported in Kaufmann et al. (2000) was used:

$$\mathrm{NDVI}\approx\frac{(1-\theta)(1-\omega_{\mathrm{NIR}}\eta_{1,\mathrm{NIR}})+\omega_{\mathrm{NIR}}\eta_{1,\mathrm{NIR}}}{(1+\theta)(1-\omega_{\mathrm{NIR}}\eta_{1,\mathrm{NIR}})+\omega_{\mathrm{NIR}}\eta_{1,\mathrm{NIR}}},\tag{22}$$

where θ is the ratio between leaf albedos at red and NIR wavelengths, i.e., $\theta=\omega_{\mathrm{red}}/\omega_{\mathrm{NIR}}$. It follows directly from Eq. (22) that $\omega_{\mathrm{NIR}}\eta_{1,\mathrm{NIR}}\approx 1-(\theta\cdot\mathrm{SR})^{-1}$. In the case of dense canopies, the ASSI, introduced in Zhang et al. (in press) can be approximated by the SR.

The ASLI was introduced to quantify the anisotropy of radiation reflected by vegetation. For a linearized signature, this variable can be evaluated as

$$\begin{aligned}\mathrm{ASLI} &= \int_{\theta_{\min}}^{\theta_{\max}}\sqrt{\left(\frac{\mathrm{dBRDF}_{\mathrm{red}}}{\mathrm{d}\mu}\right)^2+\left(\frac{\mathrm{dBRDF}_{\mathrm{NIR}}}{\mathrm{d}\mu}\right)^2}\,\mathrm{d}\mu\\ &= \sqrt{1+k^2}\int_{\theta_{\min}}^{\theta_{\max}}\left|\frac{\mathrm{dBRDF}_{\mathrm{red}}}{\mathrm{d}\mu}\right|\mathrm{d}\mu. \end{aligned}\tag{23}$$

In Eq. (23), μ is the distance introduced in Zhang et al. (in press). Thus, the ASLI is determined by variation in the shape of BRDF, which is mainly determined by the wavelength-independent probability density function F whose shape is governed by the composition, density, and geometric structure of vegetation canopies. It will be shown in Section 4 that F is the bidirectional gap probability function.

3. Signatures of vegetation in the case of a reflective ground

The three-dimensional radiation field in a scattering and absorbing medium bounded at the bottom by a reflecting surface can be expressed in terms of the ground reflectance properties (which are independent of medium) and solutions of two independent subproblems: the radiation field calculated for the case of a completely absorbing surface below the medium and the radiation field in the same medium generated by anisotropic wavelength-independent sources located at the bottom of the medium (Knyazikhin et al.,

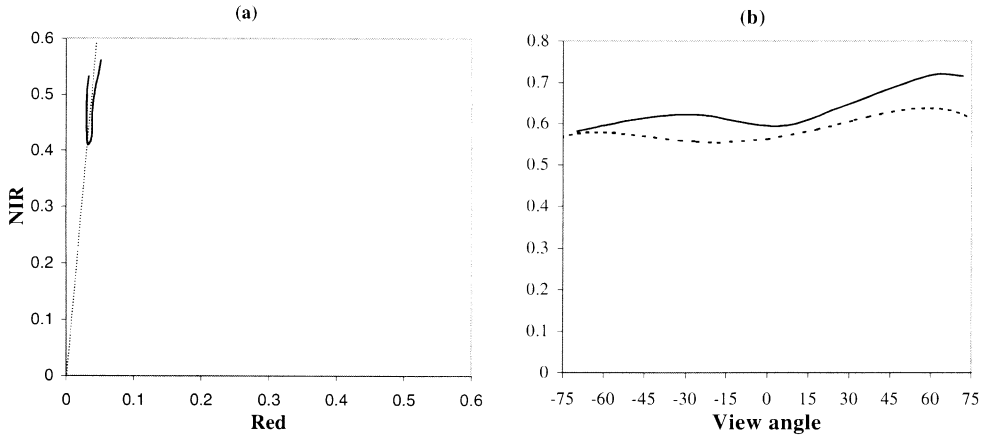

Fig. 4. (a) Angular signature of grasses derived from AirMISR data. This curve can be approximated by the liner function $\mathrm{BRDF}_{\mathrm{NIR}}=12.9\cdot\mathrm{BRDF}_{\mathrm{red}}$. The relative uncertainty $\delta\mathrm{BRDF}_{\mathrm{NIR}}/\mathrm{BRDF}_{\mathrm{NIR}}=0.17$, which does not exceed uncertainties in AirMISR surface reflectances was used. (b) Function $\omega_{\mathrm{NIR}}\eta_{1,\mathrm{NIR}}$ was derived from AirMISR data (solid line) using Eq. (19) and from the solution of the transport equation (dotted line). In model calculation, ω_{NIR} and the ratio $\theta=\omega_{\mathrm{red}}/\omega_{\mathrm{NIR}}$ were set to 0.92 and 0.22, respectively. Other parameters are the same as in Fig. 3.

1998; Marshak et al., 2000). This representation of the radiation field does not violate the law of energy conservation within the medium. For simplicity, we assume that the canopy ground can be idealized as a Lambertian surface, although this is not required for our analysis.

In the case of a reflective ground beneath the canopy, the radiative field $I_{\omega,\rho}(r,\Omega)$ in the vegetation canopy satisfies Eq. (1), boundary condition (Eq. (2)) for downward direction, and

$$I_{\omega,\rho}(r_H,\Omega) = \pi^{-1}\int_{2\pi}\rho(\Omega',\Omega)I_{\omega,\rho}(r_H,\Omega')|\mu'|d\Omega' \qquad (24)$$

for upward directions. Here, ρ is the bidirectional distribution function of the ground. In the case of Lambertian surface (i.e., ρ does not depend on angular variables), the solution of the boundary value problem (Eqs. (1), (2), and (24)) can be decomposed to a linear sum of two angle-dependent functions, namely,

$$I_{\omega,\rho}(r,\Omega) = I_\omega(r,\Omega) + \mathbf{t}(\omega)\frac{\rho}{1-\rho\mathbf{r}^*(\omega)}J_\omega(r,\Omega). \qquad (25)$$

Here, I_ω is the solution of the "black soil" problem (Eqs. (1)–(3)) discussed previously, $\mathbf{t}(\omega)$ is determined by Eq. (9) and does not depend on Ω, and J_λ and the angle-independent variable $\mathbf{r}^*(\omega)$ are radiance and downward flux at the ground level, respectively, generated by the isotropic source located at the bottom of the canopy. The function J_ω satisfies Eq. (1), zero boundary condition at the top and $J_\omega(r_H,\Omega)=\pi^{-1}$ at the bottom. The operator equation $J_\omega = \omega T J_\omega + J_S$ for J_ω can be derived by a technique analogous to that used earlier. Here, J_S is the radiance generated by photons in the isotropic source located at the bottom that have not undergone any interactions in the canopy. It satisfies the equation $LJ_S=0$ and the boundary condition $J_S(r_0,\Omega)=0$ for downward directions and $J_S(r_H,\Omega)=\pi^{-1}$ for upward directions. Because the operator L does not depend on wavelength, the function J_S is wavelength independent, too. The solution J_ω can be represented as the sum of two components, $J_\omega = J_S + \varphi^*_\omega$ (Fig. 5), where φ^*_ω satisfies the operator equation $\varphi^*_\omega = \omega T\varphi^*_\omega + \omega T J_S$. It follows from this representation that the radiative field J_ω along upward directions can be expressed as $J_\omega = J_s + \omega T J_s/(1-\omega\eta^*_{1,\omega})$ where $\eta^*_{1,\omega} = T\varphi^*_\omega/\varphi^*_\omega$. By applying the methods outlined in the previous section, it can be shown that φ^*_ω possesses properties similar to the solution of Eq. (5) in the sense of an adjoint formulation; that is, φ^*_ω along the upper (lower) canopy boundary in upward (downward) directions behaves as φ_ω at the canopy bottom (canopy top) in downward (upward) directions.

It follows from Eq. (25) that the hemispherically integrated surface reflectance $\mathbf{r}_{\omega,\rho}$ can be expressed as

$$\mathbf{r}_{\omega,\rho} = \mathbf{r}(\omega) + \mathbf{t}(\omega)\frac{\rho}{1-\rho\mathbf{r}^*(\omega)}\mathbf{t}^*(\omega) \qquad (26)$$

where $\mathbf{r}(\omega)$ is determined by Eq. (9) and $\mathbf{t}^*(\omega)$ is the upward flux at the upper canopy boundary resulting from the source located beneath the canopy. Eq. (26) determines the location of surface reflectance data in the spectral space. Decompositions (Eqs. (25) and (26)) hold true for non-Lambertian surface also. In general case, ρ is an effective ground reflectance. J_ω describes the radiative field in the vegetation canopy generated by an anisotropic wavelength-independent source located at the bottom of the canopy, the specification of which depends on the anisotropy of the canopy ground (Knyazikhin et al., 1998).

The representation Eq. (25) allows us to define biomes in terms of three basic variables that determine the radiative

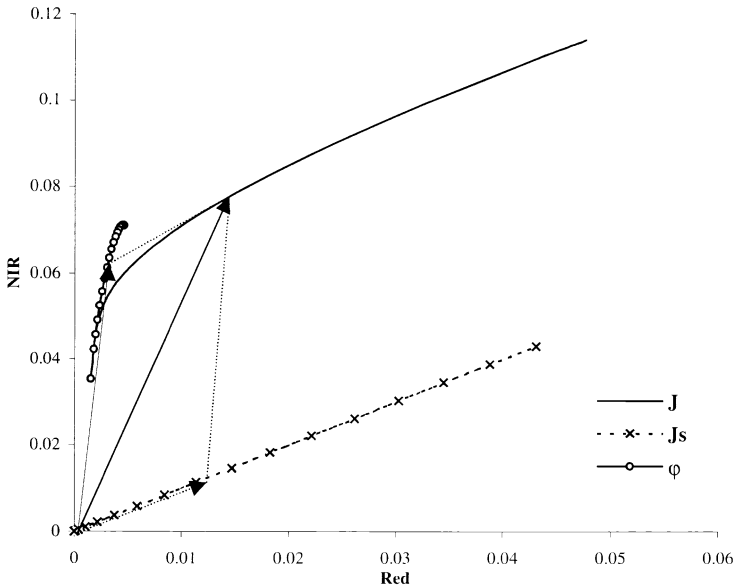

Fig. 5. Angular variation of $J_\omega(r_0,\Omega)$ (legend "**J**") on the red–NIR plane. Each point on this signature can be regarded as a vector $\boldsymbol{J}=(J_{\omega_{red}},J_{\omega_{NIR}})$, which is the sum of two vectors, **Js** = (J_S,J_S) and $\varphi = (\varphi^*_{\omega_{red}},\varphi^*_{\omega_{NIR}})$. Calculations were performed for the homogeneous canopy described in Fig. 1.

regime in vegetation canopies. They are (1) architecture of the individual plant or tree and the entire canopy, (2) optical properties of the vegetation elements, and (3) anisotropy and optical properties of the ground beneath the canopy. Indeed, I_ω and J_ω depend on leaf albedo and two wavelength-independent canopy-specific variables, p_0 and $p_{\mathbf{t}}$, both being determined by the wavelength-independent operator $\boldsymbol{T}$ (see Eqs. (7)–(15)). In addition, the anisotropy of the ground influences the behavior of J_ω whose contribution can be explicitly separated in terms of the functions J_s and $\eta^*_{1,\omega}$. The effective ground reflectance ρ in Eq. (25) describes the optical properties of the ground beneath the canopy. It follows from Eqs. (26), (15), and (11) that four wavelength-independent and vegetation structure-specific variables p_0, $p_{\mathbf{t}}$, $\mathbf{t}(\alpha)$, and $\mathbf{a}(\alpha)$, and wavelength-dependent leaf albedo and effective ground reflectance uniquely determine the location of remotely sensed surface reflectance data in the spectral space.

Eq. (25) includes two extreme situations. The first is the case of a dense canopy, which transmits a negligible amount of radiation, i.e., $J_\omega(r_0,\Omega)\mathbf{t}(\omega)\approx 0$. The angular signature of the canopy reflectance behaves as described previously. This is also the case when the surface underneath the canopy is sufficiently dark, i.e., $\rho_\lambda \approx 0$. Broadleaf forests are an example of such a situation. The second situation is characteristic of a sparse canopy, which transmits almost all incident radiation, i.e., $\mathbf{t}(\omega)\approx 1$, and scattering from green leaves is negligible; that is, $\mathbf{r}^*(\omega)\approx 0$, $I_{\omega,\rho}\approx \rho J_\omega$. In this case, the angular signature is totally determined by the optical properties of the ground. Two angle-dependent components, I_ω and J_ω, in Eq. (25) determine the BRDF signature corresponding to intermediate scenes. The first component varies about a line passing the origin of the spectral plane. This does not hold true for J_ω (Fig. 5). A deviation of biome signature from the line passing the origin, therefore, indicates the influence of the ground beneath the canopy on canopy leaving radiation. It results in a nonzero intercept in the linear regression of the signature.

We conceive the canopy reflectance in one direction as a vector on the spectral plane. Let **BRDF**, $\mathbf{BRDF}^{\mathrm{BS}}$, and **J** be vectors whose coordinates are $I_{\omega,\rho}$, I_ω, and J_ω, respectively, at red and NIR wavelengths. These vectors depend on the view direction. We denote by K a diagonal matrix whose diagonal elements are values of $\mathbf{t}(\omega)\rho/(1-\rho\mathbf{r}^*(\omega))$ at red and NIR wavelengths. This matrix is independent of the view directions. We use the symbol $\cdot_{\mathrm{L}}$ to denote the length of a vector in the spectral plane. Let $\mathbf{BRDF}_0$ be the reflectance of a vegetation canopy with the most probable structural composition. It follows from Eq. (25) that the distance between $\mathbf{BRDF}_0$ and **BRDF** of another canopy satisfies the following inequalities

$$\begin{aligned}\|\mathbf{BRDF}_0-\mathbf{BRDF}\|_{\mathrm{L}} &\le \|\mathbf{BRDF}_0^{\mathrm{BS}}-\mathbf{BRDF}^{\mathrm{BS}}|_{\mathrm{L}}\\ &+\|\mathbf{K}_0\mathbf{J}_0-\mathbf{KJ}\|_{\mathrm{L}}\le \Upsilon_{\mathrm{BS}}+\Upsilon_{\mathrm{G}},\end{aligned}\tag{27}$$

where

$$\Upsilon_{\mathrm{BS}}=\|\mathbf{BRDF}_0^{\mathrm{BS}}-\mathbf{BRDF}^{\mathrm{BS}}\|_{\mathrm{L}},$$

$$\Upsilon_{\mathrm{G}}=\max \mathbf{t}_{\mathrm{canopy}}(\omega_\lambda)\frac{\rho_{\mathrm{canopy},\lambda}}{1-\rho_{\mathrm{canopy},\lambda}\mathrm{r}^*_{\mathrm{canopy}}(\omega_\lambda)}J_{\mathrm{canopy},\omega_\lambda}.\tag{28}$$

Here, the maximum is taken over red and NIR wavelengths and two canopies. Based on the Minkowski inequality (Bronstein & Semendyayev, 1985) and representation $J_\omega=J_{\mathrm{S}}+\varphi^*_\omega$ (Fig. 5), the following estimate of the ASLI can be derived from Eq. (25)

$$\begin{aligned}\mathrm{ASLI}&=\int_{\vartheta_{\min}}^{\vartheta_{\max}}\sqrt{\left(\frac{\mathrm{d}I_{\omega_{\mathrm{red}},\rho_{\mathrm{red}}}}{\mathrm{d}\mu}\right)^2+\left(\frac{\mathrm{d}I_{\omega_{\mathrm{NIR}},\rho_{\mathrm{NIR}}}}{\mathrm{d}\mu}\right)^2}\mathrm{d}\mu\\ &\le\sqrt{1+k^2}\int_{\vartheta_{\min}}^{\vartheta_{\max}}\left|\frac{\mathrm{d}I_{\omega_{\mathrm{red}}}}{\mathrm{d}\mu}\right|\mathrm{d}\mu\\ &+\Upsilon_{\mathrm{G}}\sqrt{1+k_{\mathrm{S}}^2}\int_{\vartheta_{\min}}^{\vartheta_{\max}}\left|\frac{\mathrm{d}\varphi^*_{\omega_{\mathrm{red}}}}{\mathrm{d}\mu}\right|\mathrm{d}\mu,\end{aligned}$$

where k_{S} is the mean ratio $J_{\mathrm{NIR}}(r_0,\Omega)/J_{\mathrm{red}}(r_0,\Omega)$. It means that the ASLI is determined by variation in the shape of the BRDF and anisotropy of ground and Υ_{G}. It follows from Eq. (28) that the brighter the background, the higher the value of the ASLI. The inequality Eq. (27) separates a circle in the spectral space with its center at $\mathbf{BRDF}_0$ in one direction and radius $R=\Upsilon_{\mathrm{BS}}+\Upsilon_{\mathrm{G}}$. Aggregating these circles over all available observation directions results in a set in the spectral space that contains the multiangle data corresponding to various realizations of biome-specific canopy structures and soil patterns. Its size is determined by the radius R and the ASSL of $\mathbf{BRDF}_0$. Fig. 4 in Zhang et al. (in press) shows the biome-specific sets derived from POLDER multiangle reflectances.

4. Validity of the transport equation for vegetation media

Our theoretical investigations are based on the assumption that the three-dimensional transport equation can describe the radiative regime in vegetation canopies. Panferov et al. (2001) recently made field measurements of canopy spectral reflectance and transmittance at two sites representative of equatorial rainforests and temperate coniferous forests to test the validity of the three-dimensional transport equation for describing the radiation regime in vegetation media. The idea behind the experiments was simple. The transport equation can be regarded as a linear

operator that assigns a three-dimensional radiation field corresponding to the incident radiation (Vladimirov, 1963). Under some general conditions, this linear operator can be uniquely specified by its eigenvalues and eigenvectors (Vladimirov, 1963). Eigenvalues are measurable parameters (Panferov et al., 2001). It was demonstrated that the theoretically derived eigenvalues (Knyazikhin et al., 1998) are consistent with those derived from measurements. Thus, the linear operator of the transport equation represents radiative transfer in vegetation media. On the other hand, it has been mentioned by many investigators that the transport equation in its original form (Ross, 1981) cannot describe certain aspects of the radiation regime in vegetation canopies because it does not account for the hot-spot effect, i.e., a very sharp delta function like maximum about the retrosolar direction (Knyazikhin et al., 1992; Kuusk, 1985; Li & Strahler, 1992; Marshak, 1989; Myneni et al., 1991; Nilson, 1991; Verstraete et al., 1990). Fig. 6 illustrates the mechanism of the hot-spot effect: photons penetrate into the canopy through gaps, interact with leaves and exit the canopy though the same gaps resulting in enhanced brightness along the retroillumination direction. We shall use this example to demonstrate the ability of the transport equation to describe the hot-spot effect correctly.

Consider the three-dimensional medium shown in Fig. 6. We use the boundary value problem for three-dimensional transport equation to describe radiative transfer in this medium, which is assumed to be bounded from below and lateral sides by an absorbing surface,

$$\Omega \cdot \nabla I(r,\Omega) + \chi(r)\sigma I(r,\Omega) = \chi(r)\frac{\sigma_S}{4\pi}\int_{4\pi} I(r,\Omega')\mathrm{d}\Omega', \tag{29}$$

$$I(r_t,\Omega) = i_0\delta(\Omega-\Omega_0), \quad n_t\cdot\Omega<0,$$
$$I(r_b,\Omega) = 0, \quad n_b\cdot\Omega<0. \tag{30}$$

Here, σ and σ_S are extinction and scattering coefficients that are assumed to be constants for ease of analysis, χ is the indicator function that takes on values 1 and 0 in the "gray" and "white" areas, respectively, r_t and r_b denote points on the top (subscript "t") and bottom and lateral (subscript "b") boundaries, n_t and n_b are outward normals to the boundary at r_t and r_b, respectively, i_0 is intensity of the incident beam, and "·" denotes scalar product of two unit vectors. The solution $I(r,\Omega)$ to this problem is the radiance at r in the direction Ω that is treated as a Schwartz distribution. The Schwartz theory distinguishes two types of functions: regular and singular distributions (Vladimirov, 1971). There is a one-to-one correspondence between "usual functions" and regular distributions, and thus, an ordinary function can be regarded as a special case of a distribution. The Dirac delta function is the simplest example of a singular distribution. No usual function can be identified with it (Vladimirov, 1971). In general, a solution of the transport equation can be expressed as a sum of regular and singular distributions. The singular summand must be separated explicitly because numerical technique cannot deal with singular distributions. The mathematical theory of Schwartz distributions applicable to the transport equation was developed by Germogenova (1986). Choulli and Stefanov (1996) recently reported that there is a one-to-one correspondence between the complicated three-dimensional structure of the medium and radiation exiting the medium. They also pointed out that this property loses its validity in the case of one- and two-dimensional media. An additional singular distribution in the solution of the three-dimensional transport equation makes this one-to-one correspondence possible. We will closely follow ideas of Germogenova and Choulli and Stefanov.

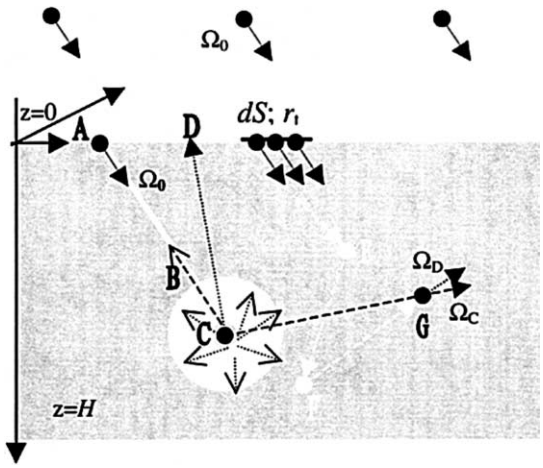

Fig. 6. Three-dimensional medium with one isolated scattering center at Point C. This medium is obtained from a homogeneous parallelepiped by removing a sphere and a line connecting the sphere and the upper medium boundary and putting a radiatively participating point at the sphere center C. The removed portion is depicted as a white area. There are no photon interactions in it. The gray area (which also includes Point C) is an absorbing and scattering medium. The direction Ω_0 of an incident beam is chosen in such way that photons can penetrate into the medium through Point A and experience the first collisions at Point C. It causes the apparition of a point diffuse source generated by photons scattered by this point. As a result, the three-dimensional radiation field decomposes into two fields. The first one is generated by the point diffuse source located at C. The second field results from photons penetrating into the canopy thorough elementary surfaces dS on the upper boundary $z=0$.

Photons entering the medium through Point A in the direction Ω_0 experience the first collision at Point C that results in the appearance of a point diffuse. It is intuitively clear that the three-dimensional radiation field decomposes into two very different fields (Fig. 6). The first is generated by this point diffuse source at C and the second from photons penetrating into the medium thorough elementary surfaces dS on the upper boundary. The incident beam, therefore, should be treated as a horizontally inhomogeneous field with respect to its contribution to the radiation regime inside the medium. We treat each point on the upper

boundary as a point monodirectional source and formulate the radiative transfer problem for each such source. The radiative response of the medium at r in direction Ω to a point monodirectional source located at r_0 is the Green's function, $G(r,\Omega;r_0,\Omega_0)$ (Bell & Glasstone, 1970), which satisfies Eq. (29) and $G(r_t,\Omega;r_0,\Omega_0)=\delta(r_t-r_0)\cdot\delta(\Omega-\Omega_0)$. The solution to the problem (Eqs. (29) and (30)) can be expressed as an integral over the upper boundary of the Green's function as

$$I(r,\Omega)=i_0\int G(r,\Omega;r_0,\Omega_0)|n_t\cdot\Omega_0|\mathrm{d}r_0. \tag{31}$$

A technique to separate the singular components from Eq. (31) is based on the following result (Choulli & Stefanov, 1996; Germogenova, 1986): for three-dimensional media, radiances, G_0 and G_1, of uncollided and single-scattered photons from a point monodirectional source are singular distributions while the remaining field is described by a regular distribution G_R. The Green's function, therefore, is the sum of two singular and one regular component, i.e., $G=G_0+G_1+G_R$. Substituting this sum into Eq. (31) results in the decomposition of the solution $I(r,\Omega)$ into three terms, $I=I_0+I_1+I_R$, being integrals over the upper boundary of G_0, G_1, and G_R, respectively. Because G_R is a regular function, the third integral, I_R, is insensitive to a value of G_R at a particular point r_0, i.e., one can ignore Point A when integrating G_R over the upper boundary. It means that the contribution of multiply scattered photons entering the medium through Point A to the term I_R can be neglected (Fig. 6).

The singular nature of G_0 and G_1 makes their integrals sensitive to particular points of the upper boundary. Therefore, we perform the integration Eq. (31) over the upper boundary surface that excludes Point A and separately over Point A. The former separates photons "continuously" penetrating into the medium through elementary surfaces dS while the letter specifies the path that results in the illumination of an isolated scattering center in the medium (Fig. 6). The integration of G_0 and G_1 over the surface results in similar expressions for the uncollided and first-order scattering radiance. Thus, the sum of I_R and these two terms is the solution I_S of the boundary value problem (Eqs. (29) and (30)). Note that I_S consists of a singular (uncollided intensity) and regular (diffuse intensity) components.

The integration of G_0 and G_1 over the set of points $\{r_A\}$ results in $I_P=I_{P,0}+I_{P,1}$, where (Germogenova, 1986)

$$I_{P,0}(r,\Omega;r_C)=\frac{i_0}{|r-r_A|^2}\delta(\Omega-\Omega_0)\times\delta\left(\Omega-\frac{r-r_A}{|r-r_A|}\right)H\times(|r_A-r_C|-|r-r_C|), \tag{32}$$

$$I_{P,1}(r,\Omega;r_C)=I_0\frac{\sigma_S\exp(-\sigma\cdot\chi(r)\cdot|r-r_C|)}{4\pi|r-r_C|^2}\times\delta\left(\Omega-\frac{r-r_C}{|r-r_C|}\right). \tag{33}$$

Here, r_A and r_C denote the Cartesian coordinates of Points A and C, respectively, H is the Heaviside function, and $|r-r_C|$ is the distance between r and r_C. Thus, a formal mathematical solution to the problem (Eqs. (29) and (30)) is

$$I(r,\Omega)=I_S(r,\Omega)+I_p(r,\Omega;r_C). \tag{34}$$

The first summand, I_S, describes the three-dimensional radiation field generated by photons penetrating into the medium through elementary surfaces dS (Fig. 6) and is insensitive to the presence of the isolated scattering center C and the paths AB. We term I_S the classical solution of the transport equation (Eq. (29)). The second summand, I_P, is the radiative response of the medium to the point source that is a singular distribution. With changes in the number of isolated scattering centers, the classical solution I_S is unchanged but the singular component transforms to the sum of $I_P(r,\Omega;r_C)$ over r_C. Note that singular solutions (Eqs. (32) and (33)) express the following well-known law, namely, the radiance in vacuum decreases between two points as the second power of the distance between the points. It follows from Eqs. (32)–(34) and the relationship $-\Omega_0=(r_A-r_C)/|r_A-r_C|$ that the exitant intensity at Point A (Fig. 6) is $I(r_A,\Omega)=I_S(r_A,\Omega)+j(r_A)\delta(\Omega+\Omega_0)$, where $j(r)=i_0\sigma_S/(4\pi|r-r_C|^2)$. The second summand causes a delta function like peak in the retroillumination direction of Eq. (34), i.e., the hot-spot effect.

Let Point C in Fig. 6 completely reflect the incident radiation while the remaining "gray area" is a completely absorbing medium. The classical solution $I_S=0$, and the singular component $I_{P,1}$ take on nonzero values within the "white area." Let the number of paths AB be changed. The classical solution is insensitive to this change. The singular component $I_{P,1}$ is sensitive to only those paths that pass Point C (e.g., Line CD). Therefore, its specification is equivalent to an estimation of the probability that a scattering center can be simultaneously viewed from two different points, i.e., the bidirectional gap probability function. This function appears in most vegetation radiation models (Kuusk, 1985; Li & Strahler, 1992; Nilson, 1991; Verstraete et al., 1990). The bidirectional gap probability, however, was not related to the solution of the transport equation previously, and thus, its incorporation into a particular model on an ad hoc basis led to the violation of the energy conservation law (Knyazikhin et al., 1998).

5. Concluding remark

The insights gained from present land cover classification activities suggest integration of multiangle data into classification attempts for future progress. Land cover types that exhibit distinct signatures in the space of remote sensing data facilitate unambiguous identification of cover types. In this two-part series, we develop a theme for consistency between cover type definitions, uniqueness of their signatures, and physics of the remote sensing data. Radiative transfer best explains the physics of the processes operative in the generation of the signal in the optical remote sensing data. Biome definitions given in terms of variables that the transport theory admits provide the basis for the consistency principle. The underlying physical principle is the energy conservation law. The three-dimensional transport equation expresses this law in the most general form. The realization of the consistency principle, therefore, means that the law of energy conservation is the required basis for a theory of land cover identification.

Acknowledgments

This research was funded by the NASA MODIS and MISR programs. We thank John Martonchik for comments on the manuscript.

References

Bell, G. I., & Glasstone, S. (1970). *Nuclear reactor theory*. New York: Van Nostrand Reinhold.

Bronstein, I. N., & Semendyayev, K. A. (1985). *Handbook of mathematics*. Berlin: Springer.

Choulli, M., & Stefanov, P. (1996). Reconstruction of the coefficient of the stationary transport equation from boundary measurements. *Inverse Problems*, *12*, L19–L23.

Diner, D., Beckert, J. C., Reilly, T. H., Brueggle, C. J., Conel, J. E., Kahn, R.A, Martonchik, J. V., Ackerman, T. P., Davis, R., Gerstl, A. A. W., Gordon, H. R., Muller, J. -P., Myneni, R. B., Sellers, P. J., Pinty, B., & Verstraete, M. M. (1998). Multi-angle imaging spectroradiometer (MISR) instrument description and experiment overview. *IEEE Transactions on Geoscience and Remote Sensing*, *36*, 1072–1087.

Diner, D. J., Barge, L. M., Bruegle, C. J., Chrien, T. G., Conel, J. E., Eastwood, M. L., Garcia, J. D., Hernandez, M. A., Kurzweil, C. G., Ledeboer, W. C., Pignatano, N. D., Sarture, C. M., & Smith, B. G. (1998). The airborne multi-angle imaging spectroradiometer (AirMISR): instrument description and first results. *IEEE Transactions on Geoscience and Remote Sensing*, *36*, 1339–1349.

Germogenova, T. A. (1986). *The local properties of the solution of the transport equation*. Moscow: Nauka (in Russian).

Justice, O., Vermote, E., Townshed, J. R. G., Defries, R., Roy, D. P., Hall, D. K., Salomonson, V. V., Privette, J. L., Riggs, G., Strahler, A., Lucht, W., Myneni, R. B., Knyazikhin, Y., Running, S. W., Nemani, R. R., Wan, Z., Huete, A. R., van Leeuwen, W., Wolfe, R. E., Giglio, L., Muller, J. -P., Lewis, P., & Barnsley, M. J. (1998). The moderate resolution imaging spectroradiometer (MODIS): land remote sensing for global research. *IEEE Transactions on Geoscience and Remote Sensing*, *36*, 1228–1249.

Kaufmann, R. K., Zhou, L., Knyazikhin, Y., Shabanov, N. V., Myneni, R. B., & Tucker, C. J. (2000). Effect of orbital drift and sensor changes on the time series of AVHRR vegetation index data. *IEEE Transactions on Geoscience and Remote Sensing*, *38*, 2584–2597.

Knyazikhin, Y. (1990). On the solvability of plane-parallel problems in the theory of radiation transport. *USSR Computer Methods and Mathematical Physics*, *30*, 557–569 (in Russian, translated into English in 1991, pp. 145–154).

Knyazikhin, Y., & Marshak, A. (1991). Fundamental equations of radiative transfer in leaf canopies and iterative methods for their solution. In: R. B. Myneni, & J. Ross (Eds.), *Photon–vegetation interactions: applications in plant physiology and optical remote sensing* (pp. 9–43). New York: Springer-Verlag.

Knyazikhin, Y., Marshak, A., & Myneni, R. B. (1992). Interaction of photons in a canopy of finite dimensional leaves. *Remote Sensing Environment*, *39*, 61–74.

Knyazikhin, Y., Martonchik, J. V., Myneni, R. B., Diner, D. J., & Running, S. (1998). Synergistic algorithm for estimating vegetation canopy leaf area index and fraction of absorbed photosynthetically active radiation from MODIS and MISR data. *Journal of Geophysical Research*, *103*, 32257–32275.

Krasnoselskii, M. A. (1964). Positive solutions of operator equations. In P. Noordhof, & S. G. Krein (1972 Eds.), *Functional analysis* (378 pp.). Groningen: Wolters-Noordhoff.

Kuusk, A. (1985). The hot-spot effect of a uniform vegetative cover. *Soviet Journal of Remote Sensing*, *3*, 645–658.

Li, X., & Strahler, A. H. (1992). Geometrical–optical bidirectional reflectance modeling of the discrete crown vegetation canopy: effect of crown shape and mutual shadowing. *IEEE Transactions on Geoscience and Remote Sensing*, *30*, 276–292.

Lucht, W., & Schaaf, C. B. (2000). An algorithm for retrieval of albedo from space using semiempirical BRDF models. *IEEE Transactions on Geoscience and Remote Sensing*, *38*, 977–998.

Marshak, A. (1989). Effect of the hot spot on the transport equation in plant canopies. *Journal of Quantitative Spectroscopy & Radiative Transfer*, *42*, 615–630.

Marshak, A., Knyazikhin, Y., Davis, A., Wiscombe, W., & Pilewskie, P. (2000). Cloud–vegetation interaction: use of normalized difference cloud index for estimation of cloud optical thickness. *Geophysical Research Letters*, *27*, 1695–1698.

Martonchik, J. V., Diner, D. J., Pinty, B., Verstraete, M. M., Member, IEEE, Myneni, R. B., Knyazikhin, Y., Gordon, H. R. (1998). Determination of land and ocean reflective, radiative, and biophysical properties using multiangle imaging. *IEEE Transactions on Geoscience and Remote Sensing, 36*, 1266–1281.

Myneni, R. B. (1991). Modeling radiative transfer and photosynthesis in three-dimensional vegetation canopies. *Agricultural and Forest Meteorology*, *55*, 323–344.

Myneni, R. B., Marshak, A., & Knyazikhin, Y. (1991). Transport theory for a leaf canopy of finite-dimensional scattering centers. *Journal of Quantitative Spectroscopy & Radiative Transfer*, *46*, 259–280.

Nicodemus, F. E., Richmond, J. C., Hsia, J. J., Ginsberg, I. W., & Limperis, T. (1977). Geometrical considerations and nomenclature for reflectance (NBS Monograph No. 160, 52 pp.). National Bureau of Standards, U.S. Department of Commerce.

Nilson, T. (1991). Approximate analytical methods for calculating the reflection functions of leaf canopies in remote sensing application. In: R. B. Myneni, & J. Ross (Eds.), *Photon–vegetation interactions: applications in plant physiology and optical remote sensing* (pp. 161–190). New York: Springer-Verlag.

Panferov, O., Knyazikhin, Y., Myneni, R. B., Szarzynski, J., Engwald, S., Schnitzler, K. G., & Gravenhorst, G. (2001). The role of canopy structure in the spectral variation of transmission absorption of solar radiation in vegetation canopies. *IEEE Transactions on Geoscience and Remote Sensing*, *39*, 241–253.

Richtmyer, R. D. (1978). *Principles of advanced mathematical physics*, *vol. 1*. New York: Springer-Verlag (422 pp.).

Riesz, F., & Sz.-Nagy, B. (1990). *Functional analysis*. New York: Dover.

Ross, J. (1981). *The radiation regime architecture of plant stands.* Norwell, MA: Dr. W. Junk (391 pp.).

Verstraete, M. M., Pinty, B., & Dickenson, R. E. (1990). A physical model of the bidirectional reflectance of vegetation canopies: 1. Theory. *Journal of Geophysical Research*, *95*, 11765–11775.

Vladimirov, V. S. (1963). *Mathematical problems in the one-velocity theory of particle transport* (Technical Report AECL-1661). Chalk River, Ontario: Atomic Energy of Canada.

Vladimirov, V. S. (1971). *Equations of mathematical physics.* New York: Marcel Dekker (418 pp.).

Wang, Y., Zhang, Y., Tian, Y., Knjazikhin, Y., Fidellow, J., & Myneni, R. B. (1999). *Radiative transfer based synergistic MODIS/MISR algorithm for the estimation of global LAI and FPAR* (MODIS Semi-Annual Report: July 1, 1999 to December 31, 1999).

Zhang, Y., Tian, Y., Myneni, R. B., & Knyazikhin, Y. (2001). Assessing the information content of multiangle satellite data for mapping biomes. 1: statistical analysis. *Remote Sensing of Environment* (accepted September 2001).